Journal of Inflammation Research

Dovepress
open access to scientific and medical research

Open Access Full Text Article

ORIGINAL RESEARCH

Potential Roles of miRNAs in Acute Rejection for Vascularized Composite Allotransplantation

Haibo Li[1,2,*], Yuan Fang[1,2,*], Xu Li[2,*], Jingting Chen[1], Yao Xiong[1], Yongzhou Shi[3], Shengli Li[1], Lincai Ye[4], Shoubao Wang[1,*], Jianda Zhou[2,*]

[1]Department of Plastic and Reconstructive Surgery, Shanghai Ninth People's Hospital, Shanghai Jiao Tong University School of Medicine, Shanghai, People's Republic of China; [2]Department of Plastic Surgery, The Third Xiangya Hospital, Central South University, Changsha, People's Republic of China; [3]Department of Neurosurgery, Neihuang Chinese Medicine Hospital, Anyang, People's Republic of China; [4]Department of Thoracic and Cardiovascular Surgery, Shanghai Children's Medical Center, Shanghai Jiaotong University School of Medicine, Shanghai, People's Republic of China

*These authors contributed equally to this work

Correspondence: Shoubao Wang; Jianda Zhou, Email wxldragon198418@163.com; zhoujianda@csu.edu.com

Aim: The development of microsurgery has greatly advanced vascularized composite allotransplantation (VCA). However, like organ transplantation, VCA is also limited by acute rejection, and concerns regarding long-term survival and function of the transplanted graft. Therefore, it is necessary to elucidate the molecular mechanisms underlying acute rejection caused by VCA, in order to improve patient survival.

Methods: Firstly, we used Brown Norway rats and Lewis rats to construct animal model of VCA. Regularly record the appearance changes of all subjects. Specimens were collected for histological examination, microRNAs (miRNAs) sequencing and RT-qPCR verification when acute immune rejection occurred. Then, bioinformatics analysis was employed to predict miRNA related molecules and pathway information. Finally, differentially expressed miRNAs were tested and verified.

Results: MiRNAs are small non coding RNA transcripts that regulate gene expression at the post-transcriptional level. Studies have shown that miRNAs are involved in immune regulation and several miRNAs have been identified that are potential diagnostic and prognostic biomarkers of acute rejection. In this study, we found that the expression levels of rno-miR-21-5p, rno-miR-340-5p, rno-miR-1-3p and rno-miR-195-5p are significantly associated with acute rejection following VCA.

Conclusion: This miRNA signature can potentially an auxiliary diagnostic indicator of rejection, which can help clinicians adjust the immunosuppressive program in time during acute rejection.

Keywords: vascularized composite tissue allograft$_1$, VCA$_2$, miRNAs$_4$, acute rejection$_5$

Introduction

Vascularized composite allotransplantation (VCA) refers to the transplantation of multiple tissues, such as skin, muscles, connective tissues, etc., as one functional unit. It is primarily used to repair large-area defects that cannot be achieved by traditional reconstruction techniques. The development of microsurgery has greatly increased the application of VCA, several cases of successful hand and face VCA surgery have been reported.[1,2] Organ recipients routinely receive immunosuppressive therapy after transplantation to prevent rejection. However, some patients still experience acute rejection after immunosuppressive therapy.[3] The long-term survival and function of the transplanted tissues is a major concern in VCA surgery as well. Therefore, it is crucial to explore the molecular mechanisms underlying acute rejection in VCA. We can detect the expression of miRNAs by biopsy. This data will help doctors make a definite diagnosis and rescue so as to reduce complications and improve the success rate. In future research, a drug targeting miRNAs can be developed to regulate mRNA expression in combination with specific miRNAs, so as to exert therapeutic effects.

Several microRNAs (miRNAs) have been identified as diagnostic/prognostic biomarkers and therapeutic targets for various diseases.[4,5] MiRNAs are a small single stranded noncoding RNA molecules consisting of 19–25 nucleotides. They regulate the expression of target messenger RNAs (mRNAs) post-transcriptionally by binding to and inhibiting

Received: 29 July 2022
Accepted: 20 October 2022
Published: 28 October 2022

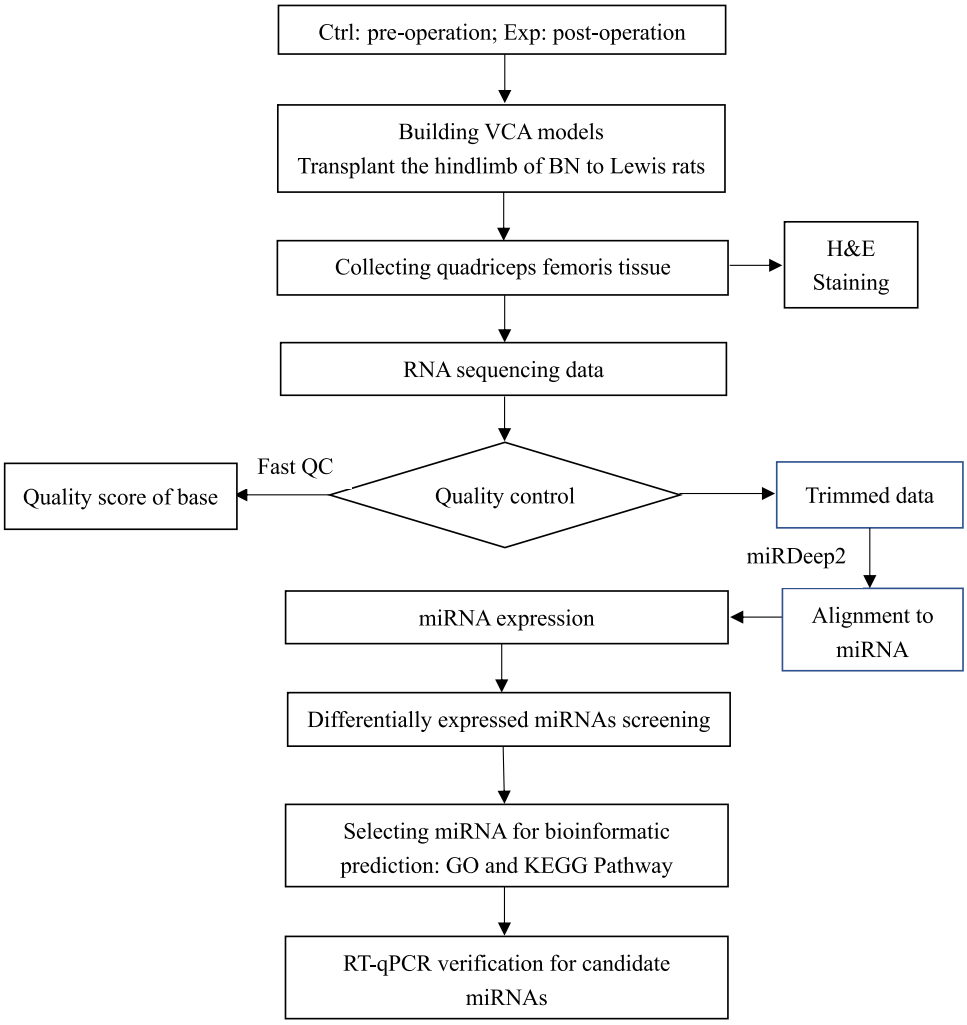

Figure 1 miRNA-sequences experiment workflow.

their translation.[6,7] Multiple miRNAs can act on one mRNA,[8] and a single miRNA can target multiple genes. Although miRNAs associated with immune rejection and immune tolerance have been identified in recent year,[9,10] little is known regarding the role of miRNAs in post-VCA acute rejection.

To this end, we established a rodent model of VCA, and analyzed the expression profiles of the miRNAs in order to gain insights into the molecular mechanisms involved in acute rejection. The flow chart of this study is shown in Figure 1.

Methods and Materials

Animals

A rodent hindlimb allograft model was constructed to simulated VCA. Four male Lewis and four male Brown Norwegian rats weighing 200–250g were purchased from Shanghai Sippr-BK Laboratory Animal Co. Ltd. (Shanghai, China). The Brown Norwegian rats were donor, the Lewis rats were recipients. The hindlimb of Lewis rat received graft from the Brown Norwegian rat. The control groups were original limbs of recipients before operation, and the experimental groups were transplanted. We compared them between the pre-operation and post-operation. All animal procedures were approved by the ethics committee of the Ninth People's Hospital Affiliated to Shanghai Jiao Tong University School of Medicine, and performed according to the guidelines of the Laboratory Animal Manual of NIH Guideline to the Care and Use of Animal.

Surgery Operation

The rats were deeply anesthetized with isoflurane and hindlimb transplantation was performed as previously described.[11] Briefly, the two hind limbs of the donor rats were perfused with cold heparinized Ringer's lactate solution, amputated in the middle of the thigh, and transplanted into the recipient rats. The femur was fixed with 18G intramedullary needle, and the dorsal muscles and skin were sutured with 3–0 silk thread. Then the femoral artery, vein and sciatic nerve were anastomosed with 12–0 nylon thread under the operating microscope. After confirming that the anastomotic vessels were unobstructed, the ventral muscles and skin were sutured with 3–0 silk thread. Motor and sensory functions were not evaluated in this study.

Histological Examination

Muscle tissues were stained with hematoxylin and eosin (H&E) stains, and were evaluated histologically according to Büttemeyer grading system for muscle rejection.[12] Normal muscle was graded as 0. Grade I rejection is characterized by patchy focal mild mononuclear interstitial infiltrates without muscle necrosis constituted, grade II consists of progressive increase in the number of mononuclear cells between the myositis and perivascular regions, and grade III rejection additionally shows aggressive lymphocytic infiltration, muscle necrosis, endothelitis and interstitial edema, which culminates in partial fibrosis of the necrotic muscle tissue.

Library Preparation

Total RNA was isolated from the muscle tissues and quantified on the NanoDrop ND-100 after confirming the integrity through agarose gel electrophoresis. The samples were subjected to 3'-amino-deacylation and 3'-cP (2',3'-cyclic phosphate) removal for 3'-adaptor ligation, and 5'-OH (hydroxyl group) phosphorylation to 5'-P for 5'-adaptor ligation. In addition, the m1A and m3C residues were demethylated to improve reverse transcription. The pretreated total RNA of each sample was used for miRNA-seq library preparation. The library was prepared using the NEBNext® Multiplex Small RNA Library Prep Set for Illumina® on the NanoDrop ND-1000 Agilent 2100 Bioanalyzer. Following 3'-adapter and 5'-adapter ligation, the RNA samples were reverse transcribed to cDNA and amplified by PCR. The ~134–160bp amplified fragments were selected and the reads were aligned to miRNA reference sequences using miRDeep2, allowing for only 1 mismatch.[13] The expression levels of the miRNAs were calculated based on the mapped read count. The differentially expressed miRNAs were screened based on the count value using R package edgeR.[14]

Sequencing Procedures

The DNA fragments were denatured with 0.1M NaOH to generate single-stranded DNA molecules, and loaded onto the reagent cartridge at the concentration of 1.8pM. The sequencing run was performed on NextSeq system using NextSeq 500/550 V2 kit (#FC-404-2005, Illumina) according to the manufacturer's instructions. Fifty sequencing cycles were run.

Bioinformatics Analysis

The target genes of the miRNAs were predicted using the miRDB database, and functionally annotated by Gene Ontology (GO) and Kyoto Encyclopedia of Genes and Genomes (KEGG) pathway enrichment analyses. The GO terms are divided into the biological processes, cellular components and molecular functions. The significantly enriched GO terms and KEGG pathways were identified on the basis of $p \leq 0.05$.

RT-qPCR

cDNA was synthesized with a cDNA synthesis kit. Fill each suitable slot on the PCR board with the sample. Place the PCR board on the real-time PCR instrument for the PCR process. The target gene and housekeeping gene of each sample were subjected to real-time PCR. The relative expression levels of the target miRNAs were normalized to that of U6 snRNA. The primer sequences utilized by our team are listed in Table 1.

Table 1 Sequences of Primers for RT-qPCR

Gene ID	Primer Sequences	Ta Opt(°C)	Product Size (bp)
U6	F:5'GCTTCGGCAGCACATATACTAAAAT3' R:5'CGCTTCACGAATTTGCGTGTCAT3'	60	89
rno-miR-21-5p	GSP:5'GCGGTAGCTTATCAGACTG3' R:5'TGCGTGTCGTGGAGTC3'	60	63
rno-miR-1-3p	GSP:5'GGGGATGGAATGTAAAGAAGT3' R:5'GTGCGTGTCGTGGAGTCG3'	60	65
rno-miR-340-5p	GSP:5'GCGGTTATAAAGCAATGAGA3' R:5' GTGCGTGTCGTGGAGTCG3'	60	66
rno-miR-195-5p	GSP:5'GGGGTAGCAGCACAGAAAT3' R:5'CAGTGCGTGTCGTGGAGT3'	60	65

Statistical Analysis

The data are presented as the mean ± standard deviation. The differentially expressed miRNAs were screened as described. The differences between groups were analyzed using the negative binomial distribution. $P \leq 0.05$ was considered statistically significant.

Results

Histological Evaluation of Allografts

Muscle fiber swelling and patchy focal mild mononuclear interstitial infiltration were observed in the allografts on the seventh day post-transplantation and classified as grade I rejection. On the tenth day post-transplantation, monocytes infiltration increased significantly and some muscle cells were necrotic, which were characteristic of Grade II rejection. Finally, diffuse lymphocyte infiltration, massive muscle fiber necrosis, and interstitial edema were observed on day 14, which corresponded to Grade III rejection (Figure 2).

Identification of Differentially Expressed miRNAs

The differentially expressed miRNAs between the control muscle tissues and transplanted allografts were identified using, and are listed in Table 2. Based on the expression levels of the samples, hierarchical clustering was performed. As shown in Figure 3A, the control and experimental samples formed distinct clusters. Changes in expression levels between

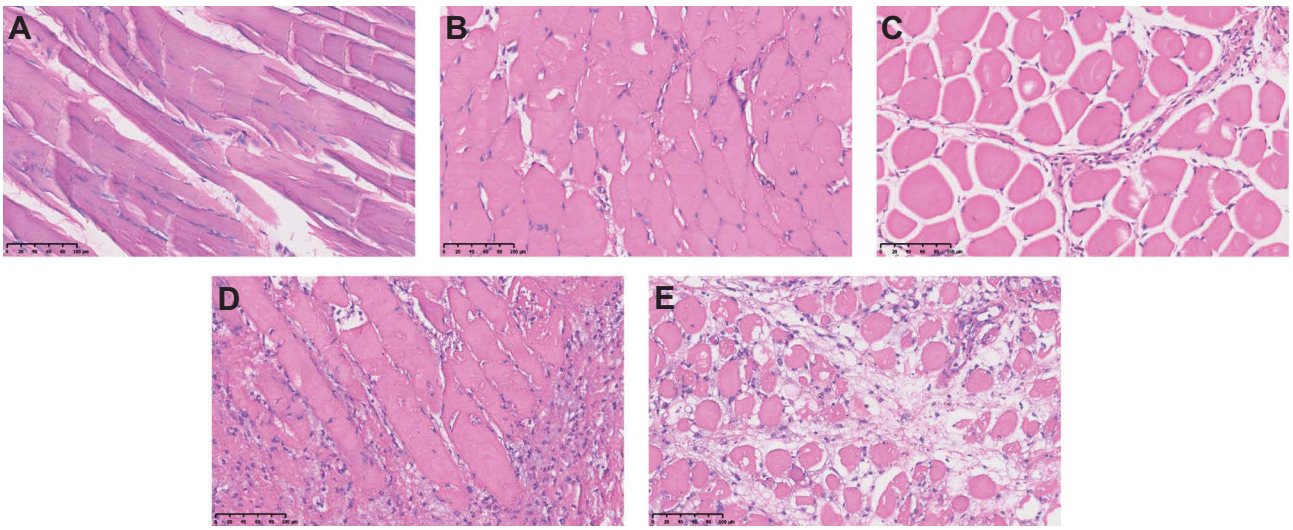

Figure 2 HE staining of muscle samples. Allograft muscle tissues at days 0 (**A**), day 3 (**B**), day 7 (**C**), day 10 (**D**) and day 14 (**E**). Bar; 100 μm.

Table 2 Differentially Expressed miRNAs

Gene_ID	Length	Fold_Change	p_value	q_value	Regulation
rno-miR-21-5p	22	33.06104206	8.39262E-38	5.30413E-35	Up
rno-miR-146b-5p	24	12.08207654	3.28153E-14	1.88539E-12	Up
rno-miR-34a-5p	22	8.292127782	1.36643E-12	6.05112E-11	Up
rno-miR-142-5p	21	7.545074812	1.43618E-12	6.05112E-11	Up
rno-miR-221-3p	23	7.418774119	1.62697E-11	5.14123E-10	Up
rno-miR-340-5p	22	5.651534972	9.46434E-11	2.30056E-09	Up
rno-miR-146a-5p	22	5.311752322	3.58435E-11	9.84917E-10	Up
rno-miR-532-5p	22	4.530594381	3.15299E-07	2.76832E-06	Up
rno-miR-20a-5p	23	4.40854251	8.65073E-09	1.13518E-07	Up
rno-miR-92a-3p	21	4.165394451	7.60367E-08	7.62781E-07	Up
rno-miR-17-5p	23	4.158452585	1.36556E-07	1.26917E-06	Up
rno-miR-16-5p	22	3.413947443	7.17567E-05	0.000348848	Up
rno-miR-140-3p	21	3.016290106	6.51991E-06	3.9621E-05	Up
rno-miR-93-5p	23	2.978023732	2.95709E-05	0.000154453	Up
rno-miR-29a-3p	22	2.874681535	3.05978E-05	0.000158507	Up
rno-miR-127-3p	22	0.097321553	3.59567E-06	2.44351E-05	Down
rno-miR-199a-3p	22	0.110936283	3.19233E-14	1.88539E-12	Down
rno-miR-434-3p	22	0.144550699	1.66594E-06	1.19645E-05	Down
rno-miR-218a-5p	21	0.178762818	6.59928E-08	6.95124E-07	Down
rno-miR-99a-5p	22	0.201702502	1.76733E-11	5.31881E-10	Down
rno-miR-145-3p	21	0.206960947	2.81277E-08	3.23212E-07	Down
rno-miR-1-3p	22	0.217891868	1.98172E-09	3.05474E-08	Down
rno-miR-195-5p	21	0.23747972	6.39571E-07	5.05261E-06	Down
rno-miR-133a-5p	22	0.240545317	7.33547E-08	7.47745E-07	Down
rno-miR-199a-5p	23	0.248347332	0.002273552	0.007522957	Down
rno-miR-499-5p	21	0.265876681	0.00011182	0.000522197	Down
rno-miR-100-5p	22	0.282543941	7.81921E-07	6.10091E-06	Down
rno-miR-195-3p	23	0.308193927	8.46017E-05	0.000408155	Down

the two sample groups were evaluated using scatter diagrams (Figure 3B). The red dots on the upper line represented miRNAs that were up-regulated, while the green dots on the lower line reflected miRNAs that were down-regulated. As shown in the volcano map in Figure 3C, there were 15 upregulated and 12 downregulated miRNAs between the two groups.

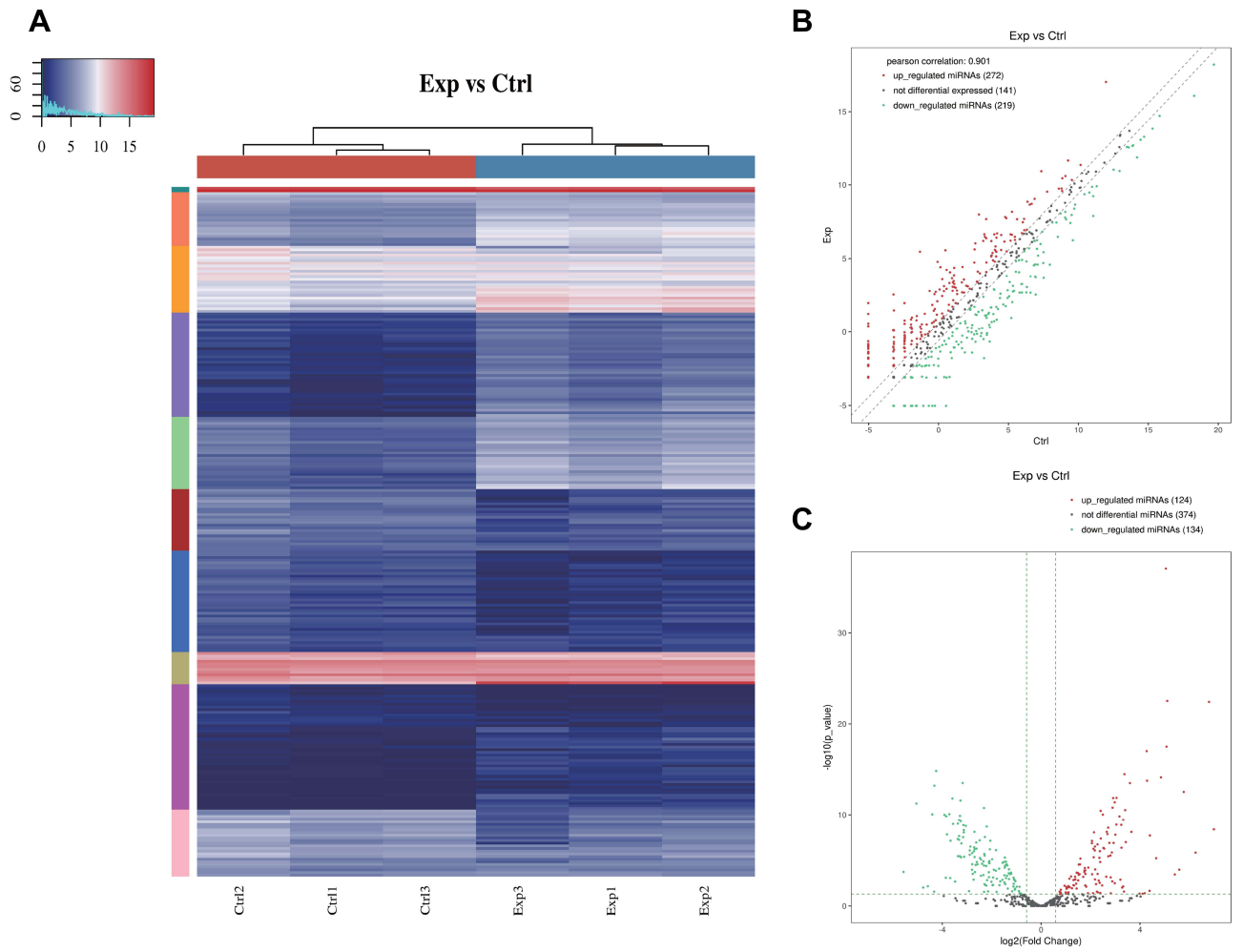

Figure 3 (**A**) The hierarchical clustering heatmap for miRNA. The color in the panel represents the relative expression level (log2-transformed). The color scale is show below: blue represents an expression level below the mean, and red represents an expression level above the mean. The colored bar top at the top panel showed the samples group, and the colored bar at the right side of the panel indicated the divisions which were performed using K-means. (**B**) The scatter plot between two groups for miRNA. The values of X and Y axes in the scatter plot are the averaged CPM values of each group (log2 scaled). miRNAs above the top line (red dots, up-regulation) or below the bottom line (green dots, down-regulation) indicate more than 1.5 fold change between the two compared groups. Gray dots indicate non-differentially expressed miRNAs. (**C**) The volcano plot of miRNA. The values of X and Y axes in the volcano Plot are log2 transformed fold change and -log10 transformed p-values between the two groups, respectively. (Red: up-regulated; Green: down-regulated). Gray circles indicate non-differentially expressed miRNAs.

Functional Prediction

The differentially expressed miRNAs were subjected to GO and KEGG analysis. The top 10 significantly upregulated miRNAs were mainly enriched in the GO terms of "intracellular" and "protein binding and developmental process" (Figure 4A). As shown in Figure 4B, the down-regulated miRNAs were mainly enriched in "Intracellular and Protein Binding", and "Regulation of Cellular". Furthermore, the up-regulated miRNAs were mainly associated with the MAPK signaling pathway, whereas the focal Adhesion signaling pathway had the highest number of target genes (Figure 4C). The Hippo pathway had the highest enrichment score and the most genes targeted by the down-regulated miRNA (Figure 4D). Therefore, we focused on this path. Among them, Hippo pathway not only had the most enriched genes, but also had a high degree of enrichment; accordingly, it became the focus of our follow-up experiments.

Verification of Differentially Expressed miRNAs

We selected 2 miRNAs that had the most target genes and maximum expression in Hippo pathway. Similarly, and two upregulated miRNAs with the most target genes in MAPK pathway for further validation by RT-qPCR. As shown in Figure 5, rno-miR-21-5p and rno-miR-340-5p were significantly upregulated, whereas rno-miR-1-3p and rno-miR-195-5p

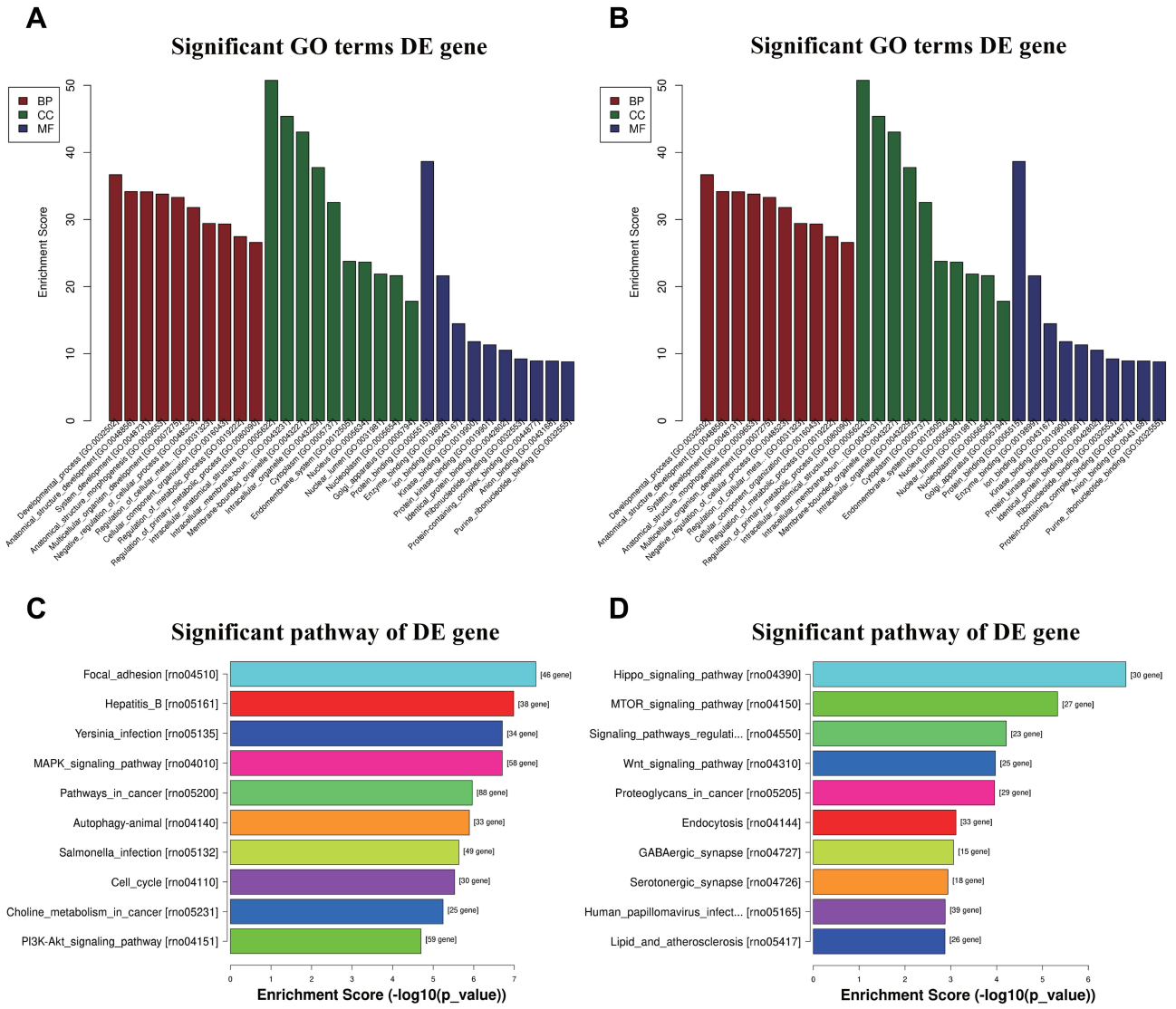

Figure 4 Bioinformatic Prediction. GO (**A**) and Pathway (**C**) analysis for up-regulated miRNA. GO (**B**) and Pathway (**D**) analysis for down-regulated miRNA.

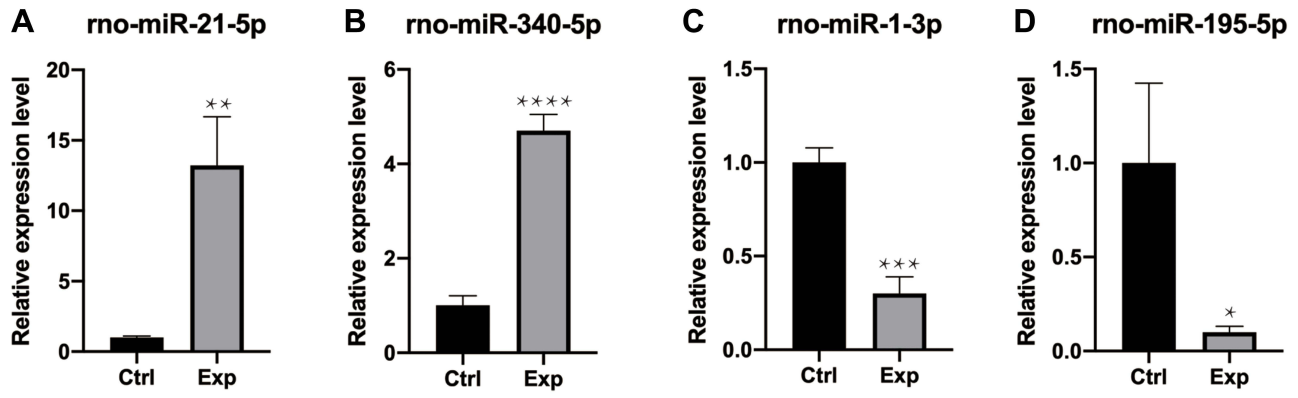

Figure 5 RT-qPCR verification. Compared with the control group (ctrl), (**A** and **B**) rno-miR-21-5p and rno-miR-340-5p were up-regulated; (**C**–**D**) rno-miR-1-3p and rno-miR-195-5p were down-regulated. The data were normalized using the mean ± standard error of the mean (SEM). *P ≤0.05, **P ≤0.01, ***P ≤0.001, ****P ≤0.0001.

showed a significant decrease in their expression levels in the allografts. The results confirmed the reliability of the sequencing data.

Discussion

Compared to organ transplantation, VCA has a higher probability of acute rejection. We previously found that early detection and timely treatment of acute rejection can improve graft survival.[11] On the other hand, delayed treatment due to lack of timely diagnosis can lead to graft loss.[15] Currently, immunosuppressive drugs are used to prolong the survival time of grafts. Therefore, it is crucial to explore mechanisms of acute rejection and prevent the deterioration of grafts from the source.

The expression levels of several plasma miRNAs were altered during acute rejection.[16] However, given the time required for the circulating miRNAs to reach the transplanted tissues, their expression levels in situ may not reflect immediate changes in the graft. Some studies have shown that pointed out that in acute rejection, the up-regulated miRNA-146a and miRNA-155 in plasma were also up-regulated in transplanted muscle tissue.[17] Yet, these were miRNAs that can be detected in plasma. In previous studies, we examined changes in skin tissue.[18] At present, the changes of muscle tissue are not clear, and few studies pay attention to the deep muscle tissue. This time, we will focus on the changes of muscle tissue in the same period.

Several studies have identified miRNAs that are aberrantly expressed in diseases, such as systemic lupus erythematosus, neurological disorders, metabolic disorders, and cancer.[19–21] They play multiple roles in various physiological processes, including neovascularization, immune regulation, and the stress response.[22,23] Therefore, it is possible that miRNAs are also involved in acute rejection during VCA. To this end, we sequenced the miRNAs in control and transplanted muscle tissues in a rodent model of VCA, and identified 28 differentially expressed miRNAs. Furthermore, the differential expression of rno-miR-21-5p, rno-miR-340-5p, rno-miR-1-3p and rno-miR-195-5p were validated by RT-PCR, and may reflect the degree of acute rejection.

VCA refers to the transplantation of multiple tissues as a functional unit. The number, state, and maturation state of antigen-presenting cells (APCs) in the different tissues determine their antigenicity, which in turn influence the degree of acute rejection. The skin was long considered to be most antigenic due to the higher numbers of APCs. However, recent studies have shown that the antigenicity in muscle is stronger than that of the skin.[24] In one study, muscle and skin tissues were separately transplanted to evaluate cell-mediated and humoral immunity. The results showed that muscle had the highest antigenicity on the 14th day after transplantation, which was also consistent with the timeline of our experimental study. Most grafts were rejected by day 7th post-transplantation and were classified as Grade I rejection. By day 14th, all samples had obvious rejection and corresponded to Grade III or complete rejection.

The Hippo signaling pathway plays an important role in immune regulation. The classic Hippo pathway is mediated YAP/TAZ, which are also the key effectors in T cell responses. TAZ promotes the fate differentiation of $CD4^+$ helper T (T_H) cells into T_H17 cells, which are the key adaptive immune cells that produce IL-17.[25] According to our transcriptomic analysis, rno-miR-1-3p and rno-miR-195-5p may play a role in acute rejection by regulating the MAPK pathway. This is the first study to assess graft rejection after VCA in terms of the muscle miRNA profiles in addition to histological evaluation. The extraction and quantification of tissue miRNAs can be completed within one day and yield results faster compared to histological evaluation. However, RNA sequencing has the disadvantage of high costs. Nevertheless, continuing advances in miRNA extraction and quantitative assessment are expected to reduce the operative costs. rno-miR-1-3p and rno-miR-195-5p can be used as auxiliary diagnostic indicator to detect acute rejection, provide a auxiliary basis for clinical diagnosis and treatment.

This study has several limitations that ought to be considered. First, the sample size was small. Nevertheless, we detected significant differences in the expression of rno-miR-1-3p and rno-miR-195-5p between tissues, which support our final conclusion. Second, we only studied muscle tissues, although vascular injuries are known to occur earlier. Third, we only selected the most significant time point (day 14) rather than multiple time points for histological evaluation and high-throughput sequencing, and may have missed potential trends. However, given the stress of tissue biopsy to the animals, it would have likely affected the accuracy of our results.

In conclusion, the expression of rno-miR-1-3p and rno-miR-195-5p expression in muscle tissues may reflect the degree of acute rejection after VCA, and are potential markers which may assist in the clinical diagnosis and treatment of VCA acute rejection.

Data Sharing Statement

The data that support the findings of this study are available on request from the corresponding author Shoubao Wang (wxldragon198418@163.com).

Acknowledgments

Thank you to all members of the Third Xiangya Hospital and Shanghai Ninth People's Hospital special support.

Funding

This work was supported by a grant from National Major Science and Technology Projects of China (2018ZX10303502), Postdoctoral Science Foundation (2019T120347) and National Natural Science Foundation of China (82002065).

Disclosure

The authors declare that the research was conducted in the absence of any commercial or financial relationships that could be construed as a potential conflict of interest.

References

1. Amaral S, Kessler SK, Levy TJ, et al. 18-month outcomes of heterologous bilateral hand transplantation in a child: a case report. *Lancet Child Adolesc Health*. 2017;1(1):35–44. doi:10.1016/S2352-4642(17)30012-3
2. Moktefi A, Hivelin M, Grimbert P, et al. Face transplantation: a longitudinal histological study focusing on chronic active and mucosal rejection in a series with long-term follow-up. *Am J Transplant*. 2021;21(9):3088–3100. doi:10.1111/ajt.16489
3. Lewis HC, Cendales LC. Vascularized composite allotransplantation in the United States: a retrospective analysis of the Organ Procurement and Transplantation Network data after 5 years of the Final Rule. *Am J Transplant*. 2021;21(1):291–296. doi:10.1111/ajt.16086
4. Fiori LM, Kos A, Lin R, et al. miR-323a regulates ERBB4 and is involved in depression. *Mol Psychiatry*. 2021;26(8):4191–4204. doi:10.1038/s41380-020-00953-7
5. Chao CT, Yeh HY, Tsai YT, Chiang CK, Chen HW. A combined microRNA and target protein-based panel for predicting the probability and severity of uraemic vascular calcification: a translational study. *Cardiovasc Res*. 2021;117(8):1958–1973. doi:10.1093/cvr/cvaa255
6. Zhang B, Chen Z, Tao B, et al. m(6)A target microRNAs in serum for cancer detection. *Mol Cancer*. 2021;20(1):170. doi:10.1186/s12943-021-01477-6
7. Lin H, Shi X, Li H, et al. Urinary Exosomal miRNAs as biomarkers of bladder Cancer and experimental verification of mechanism of miR-93-5p in bladder Cancer. *BMC Cancer*. 2021;21(1):1293. doi:10.1186/s12885-021-08926-x
8. Tang H, Yuan S, Chen T, Ji P. Development of an immune-related lncRNA-miRNA-mRNA network based on competing endogenous RNA in periodontitis. *J Clin Periodontol*. 2021;48(11):1470–1479. doi:10.1111/jcpe.13537
9. Yuan S, Chen Y, Zhang M, et al. Overexpression of miR-223 promotes tolerogenic properties of dendritic cells involved in heart transplantation tolerance by targeting Irak1. *Front Immunol*. 2021;12:676337. doi:10.3389/fimmu.2021.676337
10. Lu J, Wang X, Zhang B, Li P, Du X, Qi F. The lncRNA PVT1 regulates autophagy in regulatory T cells to suppress heart transplant rejection in mice by targeting miR-146a. *Cell Immunol*. 2021;367:104400. doi:10.1016/j.cellimm.2021.104400
11. Chen J, Wang Y, Hu H, Xiong Y, Wang S, Yang J. Adipose-derived cellular therapies prolong graft survival in an allogenic hind limb transplantation model. *Stem Cell Res Ther*. 2021;12(1):94. doi:10.1186/s13287-021-02162-7
12. Buttemeyer R, Jones NF, Min Z, Rao U. Rejection of the component tissues of limb allografts in rats immunosuppressed with FK-506 and cyclosporine. *Plast Reconstr Surg*. 1996;97(1):139–148;discussion 149–151. doi:10.1097/00006534-199601000-00023
13. Langmead B, Trapnell C, Pop M, Salzberg SL. Ultrafast and memory-efficient alignment of short DNA sequences to the human genome. *Genome Biol*. 2009;10(3):R25. doi:10.1186/gb-2009-10-3-r25
14. Robinson MD, McCarthy DJ, Smyth GK. edgeR: a Bioconductor package for differential expression analysis of digital gene expression data. *Bioinformatics*. 2010;26(1):139–140. doi:10.1093/bioinformatics/btp616
15. Moris D, Cendales LC. Sensitization and desensitization in vascularized composite allotransplantation. *Front Immunol*. 2021;12:682180. doi:10.3389/fimmu.2021.682180
16. Oda H, Ikeguchi R, Aoyama T, et al. MicroRNAs are potential objective and early biomarkers for acute rejection of transplanted limbs in a rat model. *Microsurgery*. 2017;37(8):930–936. doi:10.1002/micr.30236
17. Oda H, Ikeguchi R, Aoyama T, et al. Relative antigenicity of components in vascularized composite allotransplants: an experimental study of microRNAs expression in rat hind limb transplantation model. *Microsurgery*. 2019;39(4):340–348. doi:10.1002/micr.30408
18. Fang Y, Li H, Chen J, et al. TRFs and tiRNAs sequence in acute rejection for vascularized composite allotransplantation. *Sci Data*. 2022;9(1):544. doi:10.1038/s41597-022-01577-y
19. Singh RP, Hahn BH, Bischoff DS. Identification and contribution of inflammation-induced novel MicroRNA in the pathogenesis of systemic lupus erythematosus. *Front Immunol*. 2022;13:848149. doi:10.3389/fimmu.2022.848149

20. Sebestyen E, Nagy A, Marosvari D, et al. Distinct miRNA expression signatures of primary and secondary central nervous system lymphomas. *J Mol Diagn*. 2022;24(3):224–240. doi:10.1016/j.jmoldx.2021.11.005
21. Zhang P, Ouyang Y, Sohn YS, et al. miRNA-guided imaging and photodynamic therapy treatment of cancer cells using Zn(II)-Protoporphyrin IX-loaded metal-organic framework nanoparticles. *ACS Nano*. 2022;16(2):1791–1801. doi:10.1021/acsnano.1c04681
22. Sendi H, Yazdimamaghani M, Hu M, et al. Nanoparticle delivery of miR-122 inhibits colorectal cancer liver metastasis. *Cancer Res*. 2022;82 (1):105–113. doi:10.1158/0008-5472.CAN-21-2269
23. Yan C, Chen J, Wang C, et al. Milk exosomes-mediated miR-31-5p delivery accelerates diabetic wound healing through promoting angiogenesis. *Drug Deliv*. 2022;29(1):214–228. doi:10.1080/10717544.2021.2023699
24. Lee WP, Yaremchuk MJ, Pan Y-C, Randolph MA, Tan CM, Weiland AJ. Relative antigenicity of components of a vascularized limb allograft. *Plast Reconstr Surg*. 1991;87(3):401–411. doi:10.1097/00006534-199103000-00001
25. Dey A, Varelas X, Guan KL. Targeting the Hippo pathway in cancer, fibrosis, wound healing and regenerative medicine. *Nat Rev Drug Discov*. 2020;19(7):480–494. doi:10.1038/s41573-020-0070-z